Stimulated Emissions in Aligned CdS Nanowires at Room Temperature

Anlian Pan,[†,‡] Ruibin Liu,[†,‡] Qing Yang,[§] Yongchun Zhu,[§] Guozhen Yang,[‡,§] Bingsuo Zou,*[,†,‡] and Keqiu Chen[†]

Micro-Nano Technologies Research Center, Hunan University, Changsha 410082, China, Institute of Physics, Chinese Academy of Sciences, Beijing 100080, China, and Department of Chemistry, University of Science and Technology of China, Hefei 230026, China

Received: September 13, 2005; In Final Form: October 18, 2005

Aligned CdS nanowires (NWs) were obtained through a simple thermal evaporation process with highly active CdS nanoparticles as the evaporation source. These NWs show prominent optical waveguides behavior under a continuous-wave (CW) laser excitation. Excitation intensity-dependent photoluminescence (PL) measurements show that these NWs exhibited both broad and supernarrow stimulated emission (lasing) under intense pulse optical excitation at room temperature. Raman scattering and time-resolved PL measurements were used to investigate the optical properties. The results indicated that the stimulated emission in these NWs involves the electron−hole plasma (EHP) and Farby−Perot (F−P) optical resonant processes at room temperature.

Introduction

As a direct wide band gap (2.42 eV) semiconductor in the visible range, CdS is an excellent material used for a host of applications in optoelectronics, such as nonlinear optics and light-emitting diodes. It is also a good active optical waveguide material[1] and has electrically driven laser properties,[2] which may find wide applications in telecommunications and data storage, highly integrated chemical/biological sensors, and so on. In recent years, considerable effort has been made to study the optical pumped laser properties of 1D wide-band semiconductors for their potential wide application in micro/nanotechnologies. Yang et al.[3] first reported the room-temperature ZnO nanowire lasers in 2001. Subsequently, ZnO, GaN, and ZnS nanowire and/or nanoribbon lasings were also reported.[4−10] Compared to the nanoribbons, nanowires (NWs) seem more suitable as light propagation and photon confinement medium. Very recently, Lieber's group has observed the stimulated emission of CdS NWs at low temperature.[11] We also observed the laser emissions of wet-chemical-derived CdS NWs coated with a silica layer at room temperature,[12] while no lasing mode was detected from their bare NWs (without the silica layer) due to the lattice relaxation and poor crystallization at the surface regions. Therefore, the surface situation and crystallization play an important role in the stimulated emission properties of CdS NWs.

It was expected that lasing should occur in the highly crystallized CdS NWs with no need of a protection layer at room temperature. In addition, it is well-known that the high temperature vapor deposition method has the virtue to obtain better crystallization and cleaner products than those from the low-temperature wet-chemical route. In this work, we report the large-scale synthesis of high-quality aligned CdS NWs through a simple thermal evaporation process with highly active CdS nanoparticles as the evaporation source. These NWs show prominent optical waveguide behavior under a CW laser excitation. Stimulated emission and lasing were observed in the room-temperature PL studies of the CdS NWs.

Experimental Section

CdS NWs were synthesized on the basis of the physical evaporation of CdS nano powder with the presence of an Au catalyst. A horizontal quartz tube (inner diameter 15 mm, length 200 cm) was mounted inside a high-temperature tube furnace. An appropriate amount of CdS nanocrystalline powder (∼7 nm), prepared as described in ref 13, was placed on a ceramic plate and then loaded into the central region of the quartz tube. Next to the ceramic plate, a piece of silex coated with a layer of Au nanocrystals (∼10 nm) was placed ∼14 cm away from the boat (downstream of gas flow), and the quartz tube was introduced with high-purity He with a constant flowing rate (∼5 sccm) to eliminate the O_2 inside. After a period of time, the furnace was rapidly heated to 750 °C and maintained for several tens of minutes without changing the conditions. Then the power was switched off and the quartz tube was cooled to room temperature in the furnace. A yellow woollike product covering the substrate was obtained.

The morphology, composition, and structure of the samples were characterized by scanning electron microscopy (SEM, Hatichi S-4200) and high-resolution transmission electron microscopy (HRTEM, Philip FEG-CM 200). Optical waveguide investigation was investigated using a commercial scanning near-field optical microscopy (NSOM) from RHK Technology (USA), using the He−Cd laser (325 nm) as the excitation source. A chromatic color CCD through an objective lens was used for collecting the far-field topography and optical image. Micro-Raman experiments were conducted in a Raman scattering spectrometer (LABRAM-HR, JY, Horiba), with the 514.5 nm line of an Ar^+ laser as the excitation source. PL spectra as well as their lifetime decay profiles were measured through the following setup. Laser pulses at 793 nm (∼120 fs, 0.7 mJ, 1 kHz) were produced with a regenerative amplifier (Spitfire,

* To whom correspondence should be addressed. E-mail: zoubs@aphy.iphy.ac.cn.
† Hunan University.
‡ Chinese Academy of Sciences.
§ University of Science and Technology of China.

10.1021/jp055164m CCC: $30.25
Published on Web 12/02/2005

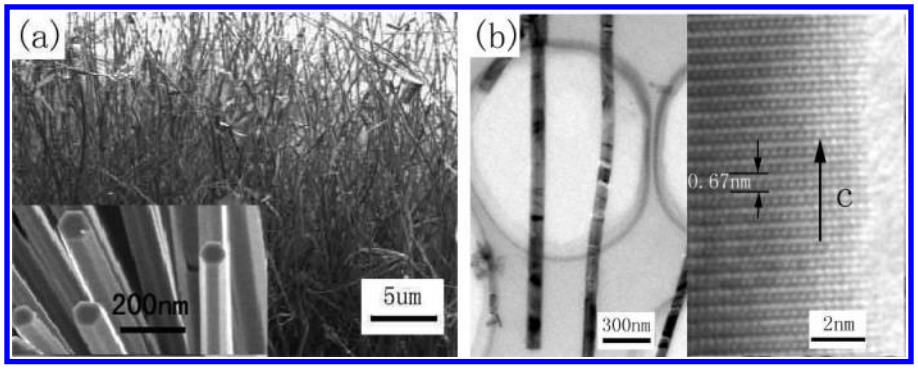

Figure 1. (a) SEM morphology of the CdS NWs (growth time, 60 min). Inset: several representative NWs in high magnification. The image at the left of (b) shows the TEM image of several CdS NWs; the right image in (b) is the HRTEM from one of the NWs.

Spectra Physics), which was seeded by a mode-locked Ti-sapphire laser (Tsunami, Spectra Physics). The produced pulses were frequency doubled in BBO to generate the second harmonic at 397 nm, which then passed through another BBO crystal and generated a mixing signal at 266 nm with a highest output power of 15 mw. Then the pulse signal was perpendicularly excited onto the surface of the sample. The output fluorescence was focused into a monochromator and detected using a photon counting streak camera (Hamamatsu C2909). The time resolution is 30 ps, and the spectral resolution of the monochromator with 150 grooves/mm grating is 0.2 nm.

Results and Discussion

The general morphology of the product (growth time, 60 min) is shown in Figure 1a. The product consists of a high density of NWs aligned predominantly perpendicular to the surface of the substrate. The inset image is the top part of several representative NWs of high magnification. The NWs have diameters ranging between 50 and 200 nm and lengths of several tens of micrometers. However, the length was only roughly estimated since the NWs are so long that a clear bird's-eye-view image could not be taken. Most of the NWs are terminated by flat hexagonal tips, which are beneficial for optical confinement as resonant cavities. The in-situ energy-dispersive X-ray spectra (EDS) indicate that only Cd and S atoms exist in the NWs and their atomic ratios are all about 1, indicating the composition of NWs is CdS. On the left of Figure 1b is the TEM image of several CdS NWs with a uniform width around 100 nm. The HRTEM from one of the NWs (right image in Figure 1b) shows that the as-prepared CdS NWs are single crystalline and the measured interplanar distance is 0.67 nm, corresponding to the (001) lattice planes of hexagonal CdS. So the growth direction of the CdS NWs is [001], along the *c* axis of the NWs.

To investigate the growth mechanism of the aligned CdS NWs, we examined the early stage of NW growth. Figure 2a shows the SEM image of the sample with a growth time of about 15 min. Many wormlike particle arrays with light-colored spherical heads were found growing upright from the substrate. The in-situ EDS (the inset in Figure 2) shows that these particles contain the elements Au, Cd, and S, which indicates that the catalytic Au nanoparticles initiated the growth of CdS NWs via the ordinary vapor−liquid−solid (VLS) growth model.[14] During the initial stage of reaction, CdS vapor was carried by He gas and deposited onto liquid Au nanoparticles. When the dissolution of CdS in the Au particles became supersaturated, short CdS nanorods extruded from the liquid Au catalysts and precipitated at the liquid−solid interface. With a longer reaction time, the dense nanorod arrays grew into aligned NWs on the

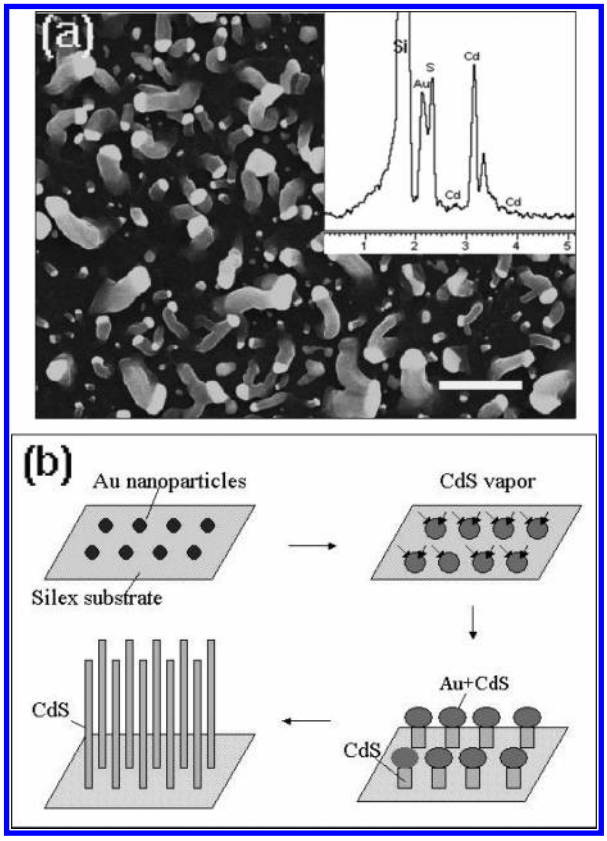

Figure 2. (a) SEM image of the sample with a growth time of about 15 min and the corresponding local EDS (inset). Scale bar: 200 nm. (b) Schematic illustration of the growth process of the aligned NWs.

substrate, which may form through a similar proximity crowding effect used to account for the formation of WO_x nanorod arrays,[15] while the catalyst particles at the top of the NWs eventually fall off from the ends of the NWs. Figure 2b shows the schematic illustration of the growth process of the aligned NWs.

Figure 3a shows a typical far-field emission image of a single CdS NW excited at the middle part with a focused laser (325 nm), which exhibits two bright emission spots at the NW ends. The long bright facula at the middle of the NW is the in-situ PL under laser excitation. A portion of the resulting PL was propagated through the NW and emitted at its ends. Figure 3b presents the near-field optical image of the upside of the NW in Figure 3a, showing that the dominant optical emission is at the tip of end, with relatively very weak emission in other regions. Figure 3c gives the position dependent optical intensity curve when the scanning probe passes across the end of the NW (the line AB shown in Figure 3b), which shows a very

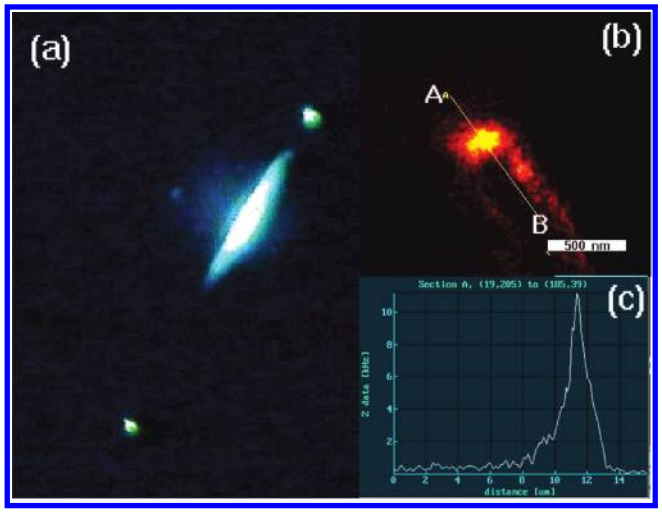

Figure 3. (a) Typical far-field emission image of a single CdS NW excited at the middle part with a focused laser (325 nm), (b) near-field optical image of the upside of the NW in (a), and (c) position-dependent optical intensity curve when the scanning probe passes across the end of the NW (line AB shown in (b)).

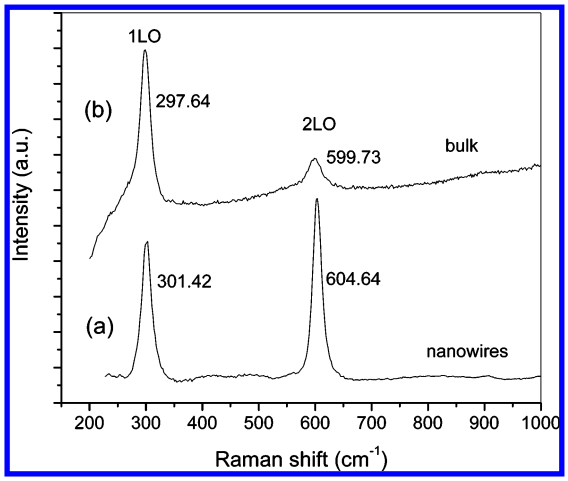

Figure 4. Room-temperature micro-Raman spectra from (a) a single NW and (b) the bulk CdS, respectively.

sharp peak at the tip of the end. The above results demonstrate that these NWs are good optical waveguide cavities.

Figure 4 shows the room-temperature micro-Raman spectra of a single NW (a) and the bulk CdS (b), respectively. The two strong peaks at ~300 and 600 cm^{-1} are attributed to the 1LO and 2LO of A_1 mode, respectively, which are polarized in the $x-z$ face and strongly couple to the exciton along c axis.[16] Interestingly, the 2LO mode is much stronger than the 1LO mode for the NWs, while the former is much weaker than the latter for the bulk CdS. Since the strength of exciton−phonon coupling in semiconductors can be assessed by the intensity ratio of overtone of phonon to the fundamental (I_{2LO}/I_{1LO}),[17,18] the extrordinary large intensity ratio of the NWs reflects a strong exciton−LO phonon coupling in these CdS NWs. This result is consistent with the conclusion of ref 16, which shows that the strength of exciton−LO phonon coupling in 1D semiconductor nanostructures can be greatly strengthened due to the phonon confinement in the transverse directions and the transfer of the elementary excitation (carriers, exciton, and phonon) in the longitudinal direction. In addition, we can see from Figure 4 that the LO mode appears at 301.42 cm^{-1} for CdS NWs and shows up at 297.64 cm^{-1} for the bulk CdS. This blueshift of LO mode by 3.78 cm^{-1} may come from the lattice contraction induced by the large surface tension in the NWs.[19]

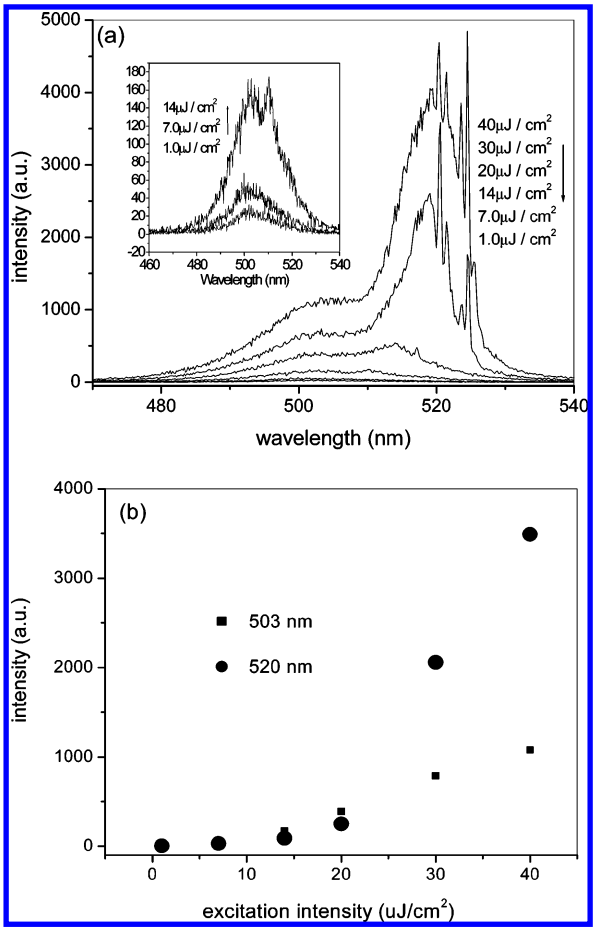

Figure 5. (a) Power-dependent PL spectra of the CdS NWs excited by femtosecond pulse (266 nm) with various excitation power densities at room temperature. The inset is the enlargement of the three curves at low excitation power for clarity. (b) Excitation power dependence of the emission intensity for spectral positions at 503 and 520 nm, respectively.

Figure 5a shows the power-dependent PL spectra of the CdS NWs excited by the femtosecond pulse (266 nm) with various excitation power densities at room temperature. At low excitation intensities a broad band appears at ~502.5 nm (2.47 eV), which is attributed to the spontaneous exciton transition at the CdS bandedge. When the excitation power increased to about 14 $\mu J/cm^2$, a new sideband appeared at the low energy side of the broad mainband. This sideband with about 37.1 meV redshift from the exciton mainband is attributed to exciton−LO phonon band (polaronic exciton band), since the LO phonon energy (ca. 38 meV) is close to the redshift and it is larger than the available thermal energy at room temperature (~26 meV).[20,21] The appearance of polaronic emission band indicates the strong exciton−phonon scattering in the CdS NWs at room temperature, which is in agreement with the conclusion of the Raman experiments (Figure 4). This strong phonon coupling would also lead to ionized carriers from the collision of excitons at high density excitation. As expected, the phonon-coupled sideband strongly redshifted and broadened when the pump power is increased to ca. 20 $\mu J/cm^2$, accompanying the increment of the emission intensity and simultaneously the appearance of some supernarrow emission lines (fwhm, ~0.4 nm). The strong redshift and broadening of the sideband is a typical characteristics of the formation of electron−hole plasma (EHP),[21,22] which comes from the interactions between phonon-coupled excitons, by the high-density excitation of the highly optical confined CdS NW cavities.

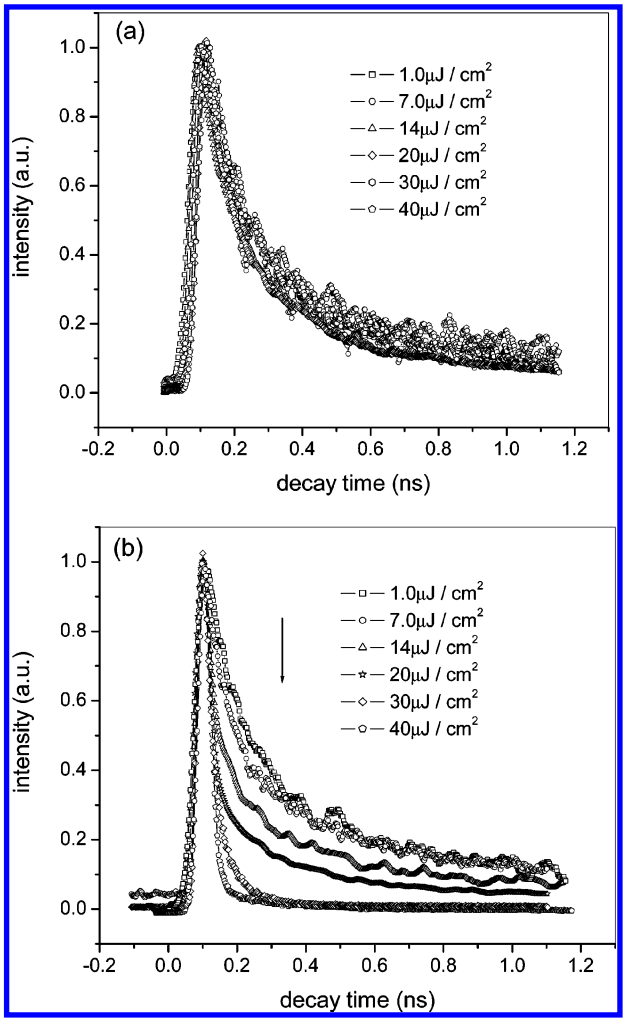

Figure 6. PL lifetime decay profiles of the emission at (a) 503 nm and (b) 520 nm respectively at different excitation powers from 1.0 to 40 μJ/cm^2.

Figure 5b plots the excitation power dependence of the emission intensity for spectral positions at 503 and 520 nm, respectively. It clearly shows that the PL intensity at 503 nm has an approximately linear increase with the rising of excitation power, whereas the emission intensity at 520 nm has a superlinear dependence of the excitation power, with a threshold at $\sim$20 μJ/cm^2. The superlinear increase in emission intensity is characteristics of amplified stimulated emission and lasing.[23] Taking these CdS NWs as F−P optical cavities, the cavity length can be calculated by formula $L = \lambda k/2n$, with n being the refractive index ($n = 2.5$ for CdS), λ the resonant wavelength (520 nm), and k an integer. The calculated cavity length is in agreement with the measured values of the CdS NWs. The adjacent line spacing ($\sim$1 nm) of the supernarrow lines (see Figure 5a) is also consistent with the calculated value using the spacing relation equation of Fabry−Perot modes,[23] indicating that these supernarrow lines come from the multimode lasing in the CdS NW cavities. Under higher intensity excitation, the amplified light emission in the optical confined NW cavities has enough gain to compensate the optical losses and leads to the appearance of these multimode lasing.

These spectral characteristics of the CdS NWs were further studied by the PL lifetime decay profiles of the emission at 503 and 520 nm respectively at different excitation powers. Figure 6 shows that the emissions at 503 nm have similar decay profiles (Figure 6a) at different excitation intensities from 1.0 to 40 μJ/cm^2, which indicates that these bands are indeed originated from the spontaneous radiation recombination of CdS,[21] while the PL lifetime decay profiles for the 520 nm band show clear pump intensity dependence (Figure 6b). The obviously shortened PL lifetimes with the increasing excitation power further confirm the occurrence of stimulated emissions in these CdS NWs.

Generally speaking, the enhanced light emission of an object corresponds to the enhanced light absorption. For nanometer-sized CdS, usually transient bleach was observed around the band gap transition. Only transient absorption occurs for the CdS NWs. The reason for the above phenomena is the difference of the confinements in both systems. For QDs, 3D confinement leads to discrete levels, which follow the state-filling effect due to Fermonic carrier population at high excitation, so optical bleaching dominates.[24] As for 1D NWs with thickness of above $2a_B$ (Bohr radius), 2D confinement take effect at x,y directions, but not at the z direction, and then the excitons behave like bosonic particles and have a giant oscillator strength [25] under laser excitation in a definite exciton phase space, so only transient absorption occurs. However, with extension of the time scale at room temperature, excitons would dissociate to form EHP due to the carrier and phonon scattering. It is the EHP process that can produce lasing under high excitation.

As discussed in ref 26, in a polar CdS semiconductor, the strong exciton−phonon coupling can lead to the formation of an Urbach band tail of states extending the energy bands into the energy gap. Our observation (Figure 5a) shows that lasing modes occur at the low-energy side of the EHP band, but almost no modes appear at the high-energy side. Hence, it is deduced reasonably that the laser emission at the high-energy side of the EHP band can, to some degree, be reabsorbed by the Urbach tail, while this reabsorption at the low-energy side cannot occur since its emission energy is far from the Urbach tail in the band gap.[26] The reabsorption process can well account for the lasing spectral distribution of the NWs (Figure 5a).

In addition, since it is difficult to keep all of NWs parallel to each other for their long length, a lot of NWs were excited simultaneously when the pulse signal was perpendicularly focused onto the CdS NW film. The persistent existing broad spontaneous emission band at about 503 nm under excitation above threshold power should result from the emissions of those non-upright NWs, which are unlikely to give optical gain and stimulated light emission for the bad detection angles. The absence of the lasing modes at some spectral position may also be caused by some of the non-upright NWs with the corresponding cavity length.

Conclusion

In summary, high-density CdS NWs were obtained through a thermal evaporation method. The structure and growth process of these NWs were investigated. The NWs show prominent optical waveguides behavior under the illumination of a CW laser. Room-temperature Raman scattering was conducted and compared with that of bulk CdS, indicating an enhanced electron−phonon coupling in the NWs. Stimulated broad and supernarrow lasing emissions under fs laser pulse excitation were observed at room temperature. The mechanism was found to involve the optical gains of both EHP and F−P processes.

Acknowledgment. The authors are grateful for the financial support of the NSFC of China (Term No. 20173073), National 973 Project, Nano and Bio-device Key Project of CAS, and 985 project of HNU.

References and Notes

(1) Barrelet, C. J.; Greytak, A. B.; Lieber, C. M. *Nano Lett*. **2004**, *4*, 1981.
(2) Duan, X.; Huang, Y.; Argarawal, R.; Lieber, C. M. *Nature* **2002**, *421*, 24.
(3) Huang, M. H.; Mao, S.; Feick, H.; Yan, H.; Wu, Y.; Kind, H.; Weber, E.; Russo, R.; Yang, P. *Science* **2001**, *292*, 1897.
(4) Qiu, Z.; Wong, K. S.; Wu, M.; Lin, W.; Xu, H. *Appl. Phys. Lett*. **2004**, *84*, 2739.
(5) Ding, J. X.; Zapien, J. A.; Chen, W. W.; Lifshitz, Y.; Lee, S. T.; Meng, X. M. *Appl. Phys. Lett*. **2004**, *85*, 2361.
(6) Johnson, J. C.; Yan, H.; Yang, P.; Saykally, R. J. *J. Phys. Chem. B* **2003**, *107*, 8816.
(7) Johnson, J. C.; Knutsen, K. P.; Yan, H.; Law, M.; Zhang, Y.; Yang, P.; Saykally, R. J. *Nano Lett.* **2004**, *4*, 197.
(8) Liu, Y. K.; Zapien, J. A.; Geng, C. Y.; Shan, Y. Y.; Lee, C. S.; Lifshitz, Y.; Lee, S. T. *Appl. Phys. Lett.* **2004**, *85*, 3241.
(9) Yan, H.; Johnson, J.; Law, M.; He, R.; Knutsen, K.; McKinney, J. R.; Pham, J.; Saykally, R.; Yang, P. *Adv. Mater*. **2003**, *15*, 1907.
(10) Johnson, J. C.; Choi, H.; Knutsen, K. P.; Schaller, R. D.; Yang, P.; Saykally, R. J. *Nat. Mater*. **2002**, *1*, 106.
(11) Agarwal, R.; Barrelet, C. J.; Lieber, C. M. *Nano Lett*. **2005**, *5*, 917.
(12) Pan, A.; Wang, S.; Liu, R.; Li, C.; Zou, B. *Small* **2005**, *1*, 1058.
(13) Pan, A. L.; Ma, J. G.; Yan, X. Z.; Zou, B. S. *J. Phys.: Condens. Matter* **2004**, *16*, 3229.
(14) Pan, Z. W.; Dai, Z. R.; Ma, C.; Wang, Z. L. *J. Am. Chem. Soc*. **2002**, *124*, 1817.
(15) Liu, J. G.; Zhao, Y.; Zhang, Z. J. *J. Phys: Condens. Matter* **2003**, *15*, 453.
(16) Arguello, C. A.; Rousseau, D. L.; Porto, S. P. S. *Phys. Rev.* **1969**, *181*, 1351.
(17) Shiang, J. J.; Risbud, S. H.; Alivisatos, A. P. *J. Chem. Phys.* **1993**, *98*, 8432.
(18) Shen, W. Z. *Physica B* **2002**, *322*, 201.
(19) Scamarcio, G.; Lugara, M.; Manno, D. *Phys. Rev. B* **1992**, *45*, 13792.
(20) Koch, S. W.; et al. *Phys. Status Solidi B* **1978**, *89*, 431.
(21) Fischer, T.; Bille, J. *J. Appl. Phys.* **1974**, *45*, 3937.
(22) Saito, H.; Gobel, E. O.*Phys. Rev. B.* **1985**, *31*, 2360.
(23) Iga, K. *Handbook of Semiconductor Lasers and Photonic Integrated Circuits*; Chapman & Hall: London, 1994.
(24) Schmitt-Rink, S.; Miller, D. A. B.; Chemla, D. S. *Phys. Rev. B* **1987**, *35*, 8113.
(25) Takagahara, T.; Hanamura, E. *Phys. Rev. Lett.* **1986**, *56*, 2533.
(26) Pan, A.; Liu, D.; Liu, R.; Wang, F.; Zhu, X.; Zou, B. *Small* **2005**, *1*, 980.